Characterization of a supercritical fluid chromatographic retention process with a large pressure drop by the temporal average density

Xin Zhang and Daniel E. Martire

Department of Chemistry, Georgetown University, Washington, DC 20057 (USA)

Richard G. Christensen

Organic Analytical Research Division, National Institute of Standards and Technology, Gaithersburg, MD 20899 (USA)

ABSTRACT

The characterization of supercritical fluid chromatographic retention by different forms of the average density, *viz.*, the temporal average density, the spatial average density and the arithmetic average density, is investigated in a system with appreciable pressure drop along the column. The logarithm of the capacity factor, when described in terms of the temporal average density, is independent of the pressure drop. Hence, supercritical fluid chromatographic retention processes can be characterized and represented by a hypothetical zero-pressure-drop system at a density equal to the temporal average density of the real system.

INTRODUCTION

In supercritical fluid chromatography (SFC), the mobile phase is highly compressible and a pressure drop necessarily exists along the column, which usually varies from around 1 bar (1 bar = $1 \cdot 10^5$ Pa) for a short capillary column, up to 30 bar for a conventional packed column and sometimes exceeding 150 bar for a column with small particles [1]. Therefore, there is always a density gradient along the length of an SFC column. As a solute band travels, it experiences varying conditions of mobile phase density; hence, the local retention may be significantly different at different positions along the column. At a specific column position, the local retention depends on the local density at that position. The local capacity factor, k', which charac-

terizes solute retention in SFC, can, in general, be expressed as a function of local density, ρ, by [2]

$$\ln k' = a + b\rho + c\rho^2 \tag{1}$$

where a, b and c are temperature-dependent quantities, independent of mobile phase density.

Eqn. 1 is a general expression for solute retention in SFC, derived from a unified theory of chromatography [2–5] and applicable to different types of SFC systems, such as those with a solid stationary phase, a fluid stationary phase or a chemically bonded stationary phase. The coefficients a, b and c may be expressed in terms of molecular interaction parameters, which correspond to the chromatographic retention mechanism involved. Therefore, the relationship between the local retention and local density, namely, the coefficients a, b and c, provide significant insight into the molecular interactions in the system to reveal the microscopic mechanism of retention. Unfortunately, but as is to be expected for

Correspondence to: Dr. D. E. Martire, Department of Chemistry, Georgetown University, Washington, DC 20057, USA.

an SFC system with a packed column, measurements of local retention and local density are usually not feasible. The experimentally measured or observed retention is an average of the local retention throughout the length of the column. In studying the physical chemistry of an SFC retention process using a packed column, a fundamental problem is to correlate the characteristic retention process with experimentally measured parameters.

Starting with Darcy's law, Martire [6] presented a generalized treatment of a packed column with a pressure drop and proposed three possible ways to express mobile phase average densities in an SFC column:

(1) Arithmetic average density,

$$\langle \rho \rangle_a = 0.5 \, (\rho_i + \rho_o) \tag{2}$$

where ρ_i and ρ_o denote the column inlet and outlet densities.

(2) Spatial average density, *i.e.*, the mobile phase density averaged over the length of the column (L),

$$\langle \rho \rangle_x = \frac{\int_0^L \rho \, dx}{\int_0^L dx} = \frac{\int_{\rho_o}^{\rho_i} \rho D_x(\rho) \, d\rho}{\int_{\rho_o}^{\rho_i} D_x(\rho) \, d\rho} \tag{3}$$

where $D_x(\rho)$ is the spatial distribution function, given by

$$D_x(\rho) = \eta^{-1} \rho \left(\frac{dP}{d\rho} \right)_T = (\eta \beta)^{-1} \tag{4}$$

where η is the viscosity of the mobile phase, P is the pressure, T is the temperature and β denotes the isothermal compressibility of the mobile phase.

(3) Temporal average density, *i.e.*, the mobile phase density averaged over the residence time (t_u) in the column,

$$\langle \rho \rangle_t = \frac{\int_0^{t_u} \rho \, dt}{\int_0^{t_u} dt} = \frac{\int_{\rho_o}^{\rho_i} \rho D_t(\rho) \, d\rho}{\int_{\rho_o}^{\rho_i} D_t(\rho) \, d\rho} \tag{5}$$

where $D_t(\rho)$ is the temporal distribution function, given by

$$D_t(\rho) = \eta^{-1} \rho^2 \left(\frac{dP}{d\rho} \right)_T = \rho(\eta \beta)^{-1} = \rho D_x(\rho) \tag{6}$$

It has also been shown [6] that the observed capacity factor is the temporal average capacity factor,

$$\langle k' \rangle_{obs} = \langle k' \rangle_t \tag{7}$$

To study the relationship between the observed retention and average density, it is reasonable to assume that the logarithm of the observed capacity factor is a quadratic function of the average mobile phase density, similar in form to the fundamental eqn. 1,

$$\ln \langle k' \rangle_{obs} = \ln \langle k' \rangle_t = a' + b' \langle \rho \rangle_y + c' \langle \rho \rangle_y^2 \tag{8}$$

where subscript y may be either t for temporal average, x for spatial average or a for arithmetic average, and a', b' and c' are the fitting coefficients at a given temperature, independent of mobile phase density.

There has not yet been a sound mathematical link between eqns. 1 and 8. Nevertheless, eqn. 8 can be regarded as a logical extension of eqn. 1 and as an empirical equation. In this experimental study, we demonstrate that the SFC retention process can be better characterized by the temporal average density than by either the frequently employed arithmetic average density or the spatial average density, and that the SFC retention process can be characterized and represented by a hypothetical zero-pressure-drop system at a density equal to the temporal average density of the real system.

EXPERIMENTAL[a]

The experiment was carried out on an HP 79887A SFC system (Hewlett-Packard, CA, USA). The system consisted of a variable-wavelength UV detector, a pump assembly with a refrigerated circulating bath which was maintained at -10 to -5°C, a back-pressure regulator which controlled the column outlet pressure, a manual injection valve and two pressure gauges for the inlet and outlet pressures of the column, respectively. The temperature control and pressure gauges of the system were carefully

---

[a] Certain commercial equipment, instruments or materials are identified in order to adequately specify the experimental procedure. This does not imply recommendation or endorsement by the National Institute of Standards and Technology.

calibrated. The temperature was controlled to within 0.2°C, and the error in the pressure readout was less than 1 bar.

The column used in this study was a silica high-performance liquid chromatography column, 25 cm × 4.6 mm I.D., 5-μm particle size. Carbon dioxide, SFC grade, was employed as the mobile phase, and benzene, methyl-, ethyl-, n-propyl- and n-butylbenzene as the probe solutes.

Since there was extra tubing between the column ends and the pressure gauges, the measured inlet and outlet pressures (the inlet and outlet pressure readouts) were different from the actual column inlet and outlet pressures. The pressure drops and the residence time of the solutes caused by this extra tubing were carefully determined through a series of calculations and by replacing the packed column by an empty column of the same diameter [7]. With these corrections, the true inlet and outlet pressures of the column, and the true solute retention times were accurately obtained.

The column void volume (V_0) was measured by a weighing method as follows: using n-hexane as the solvent to fill the dry column, the void volume was calculated by dividing the difference in the column weights (in grams, obtained before and after the solvent filling), by the density of hexane (g/ml). The void volume was measured at both the beginning and the end of the experiment and the agreement between the two measurements was within 1%. The flow-rate of the mobile phase leaving the system was measured in l/min, at ambient temperature and pressure, using a wet test flow meter. This flow-rate was converted into mass flow-rate, expressed as g of carbon dioxide/min, using the equation of state of an ideal gas. The average density of carbon dioxide, in forms of the spatial, the temporal and the arithmetic averages, was calculated by a computational program, knowing the inlet and outlet pressures, and using the Benedict–Webb–Rubin (BWR) equation of state (see ref. 8). Then, the corrected solute retention volume was obtained by the following equation:

$$V_R = \frac{t_R \cdot \dot{m}}{\langle \rho \rangle_x} \tag{9}$$

where t_R is the corrected retention time (min), $\dot{m}$ is the mass flow-rate of the mobile phase (g/min) and $\langle \rho \rangle_x$ is the spatial average density.

Ultimately, the natural logarithm of the observed capacity factor was calculated as

$$\ln \langle k' \rangle_{obs} = \ln \left(\frac{V_R - V_0}{V_0} \right) \tag{10}$$

RESULTS

In the experiments, the outlet pressure of the column was kept constant and the inlet pressure was varied by adjusting the flow-rate to generate the desired pressure drop. Some typical experimental results for ethylbenzene at various temperatures from 50 to 80°C are listed in Table I, corresponding to the calculated temporal, spatial, and arithmetic average density.

As seen in Fig. 1, plots of the logarithm of the observed capacity factor vs. the pressure drop give monotonically decreasing curves at constant outlet pressure. The decrease of the observed capacity factor with increasing pressure drop is due to the increase in the average density, in contrast to that observed with constant inlet density [9], where the average density decreases with increasing pressure drop.

Using the experimental data for ethylbenzene listed in Table I, plots of the logarithm of the observed capacity factor vs. the different forms of average density, as shown in Figs. 2–5, indicate that the logarithm of the observed capacity factor is better related to the temporal average density than to the other forms of average density, especially at the lower temperatures.

At the lower temperatures, as illustrated in Figs. 2 (at 50°C) and 3 (at 60°C), when characterized by the temporal average density, regardless of the outlet pressure, the observed capacity factor of ethylbenzene follows a continuous, smooth curve at a given temperature. However, if one of the other average densities is employed, each of the curves then splits up into two or three separate and incompatible curves corresponding to the different outlet pressures. The separation and incompatibility of the curves are even more pronounced when using the arithmetic average density than the spatial average density, due to the markedly non-linear distribution of the mobile phase density along the column [8]. The three forms of the average density have different dependencies on the mobile phase

TABLE I

LOGARITHM OF THE OBSERVED CAPACITY FACTOR OF ETHYLBENZENE

T ($^{\circ}$C)	Outlet pressure (bar)	Pressure drop (bar)	Temporal average density (g/ml)	Spatial average density (g/ml)	Arithmetic average density (g/ml)	ln $\langle k' \rangle$ ethyl-benzene
50	90	13.4	0.362	0.357	0.361	1.085
	90	18.8	0.405	0.396	0.398	0.697
	90	27.0	0.464	0.448	0.439	0.370
	90	31.2	0.493	0.475	0.457	0.178
	105	5.7	0.483	0.482	0.481	0.343
	105	11.4	0.515	0.513	0.508	0.129
	105	16.9	0.544	0.540	0.530	−0.048
	105	23.1	0.571	0.567	0.551	−0.229
	120	3.8	0.599	0.599	0.598	−0.408
	120	10.4	0.619	0.618	0.616	−0.470
	120	18.2	0.636	0.636	0.631	−0.583
	120	22.2	0.647	0.646	0.640	−0.619
	120	27.5	0.659	0.658	0.650	−0.771
60	90	13.4	0.277	0.275	0.276	1.727
	90	20.2	0.309	0.304	0.307	1.478
	90	27.0	0.399	0.331	0.335	1.206
	90	33.2	0.372	0.359	0.362	0.916
	90	39.2	0.404	0.388	0.387	0.705
	90	44.9	0.435	0.415	0.409	0.524
	90	51.7	0.467	0.444	0.430	0.350
	105	4.7	0.345	0.345	0.345	1.227
	105	12.4	0.374	0.372	0.372	0.992
	105	16.9	0.397	0.393	0.393	0.776
	105	23.2	0.427	0.421	0.419	0.567
	105	30.4	0.461	0.452	0.445	0.327
	120	6.8	0.463	0.462	0.461	0.372
	120	11.4	0.481	0.484	0.478	0.250
	120	19.0	0.509	0.507	0.502	0.077
70	90	14.4	0.240	0.239	0.239	2.085
	90	23.6	0.267	0.264	0.265	1.873
	90	27.9	0.283	0.278	0.280	1.733
	90	36.1	0.312	0.303	0.306	1.481
	90	39.9	0.329	0.319	0.321	1.314
	90	49.8	0.368	0.352	0.353	1.055
	90	55.5	0.393	0.374	0.372	0.839
	105	6.7	0.288	0.287	0.287	1.568
	105	12.4	0.303	0.302	0.303	1.423
	105	17.9	0.323	0.320	0.321	1.258
	105	25.2	0.349	0.344	0.345	1.046
	105	31.4	0.372	0.365	0.365	0.877
	105	38.4	0.399	0.390	0.388	0.678
	105	43.4	0.419	0.408	0.404	0.538
	105	49.2	0.442	0.428	0.420	0.381
	120	10.4	0.379	0.378	0.378	0.916
	120	18.9	0.407	0.405	0.404	0.697
	120	25.1	0.430	0.426	0.424	0.564

TABLE I *(continued)*

T (°C)	Outlet pressure (bar)	Pressure drop (bar)	Temporal average density (g/ml)	Spatial average density (g/ml)	Arithmetic average density (g/ml)	$\ln \langle k' \rangle$ ethyl-benzene
70	120	30.3	0.449	0.444	0.439	0.409
	120	36.6	0.470	0.463	0.456	0.270
	120	44.1	0.494	0.486	0.475	0.129
	120	53.0	0.518	0.509	0.493	−0.020
80	90	12.7	0.211	0.211	0.211	2.144
	90	18.4	0.222	0.222	0.222	2.064
	90	26.8	0.243	0.240	0.240	1.926
	90	31.1	0.255	0.251	0.251	1.779
	90	37.3	0.273	0.266	0.267	1.674
	90	43.3	0.292	0.283	0.284	1.506
	90	50.4	0.314	0.303	0.303	1.307
	90	56.2	0.334	0.320	0.319	1.114
	105	6.7	0.252	0.252	0.252	1.719
	105	13.4	0.267	0.266	0.266	1.594
	105	21.9	0.288	0.286	0.286	1.416
	105	28.2	0.306	0.302	0.302	1.277
	105	33.4	0.322	0.317	0.317	1.146
	105	40.5	0.344	0.337	0.336	0.976
	105	45.5	0.360	0.351	0.350	0.857
	105	52.2	0.383	0.371	0.368	0.681
	120	5.8	0.310	0.309	0.309	1.222
	120	10.4	0.321	0.320	0.320	1.125
	120	19.2	0.343	0.342	0.341	0.976
	120	26.3	0.364	0.361	0.360	0.809
	120	29.5	0.375	0.372	0.370	0.713
	120	36.6	0.396	0.390	0.388	0.576
	120	43.6	0.417	0.410	0.405	0.431
	120	50.5	0.437	0.428	0.421	0.337

density distribution. The temporal average density is the most sensitive to the density distribution while the arithmetic average density is totally independent of the density distribution. Therefore, when the density distribution of the mobile phase is highly non-linear, use of the arithmetic average density to characterize SFC retention will result in the largest errors.

At the higher temperatures, as illustrated in Figs. 4 (at 70°C) and 5 (at 80°C), the interesting differences in the characterization using the different forms of average density disappear, and all three forms are equally good in correlating the logarithm of the observed capacity factor of ethylbenzene. The reason is that, for a specific pressure drop, the density gradient along the column is a function of tempera-

ture, and it is smaller at high temperature (*i.e.*, when the temperature is much higher than the critical temperature) than at low temperature (*i.e.*, when the temperature is closer to the critical temperature, where the density strongly depends on the pressure). Thus, when the temperature is high, the arithmetic average density, the spatial average density and the temporal average density become nearly identical.

It has been reported that at constant mean density of the mobile phase, the observed retention is a function of the pressure drop of the system [9,10]. However, it should be noted that the reported experiment was carried out at constant arithmetic average density rather than constant temporal average density. Because the mobile phase spends relatively more time in the high density region of the
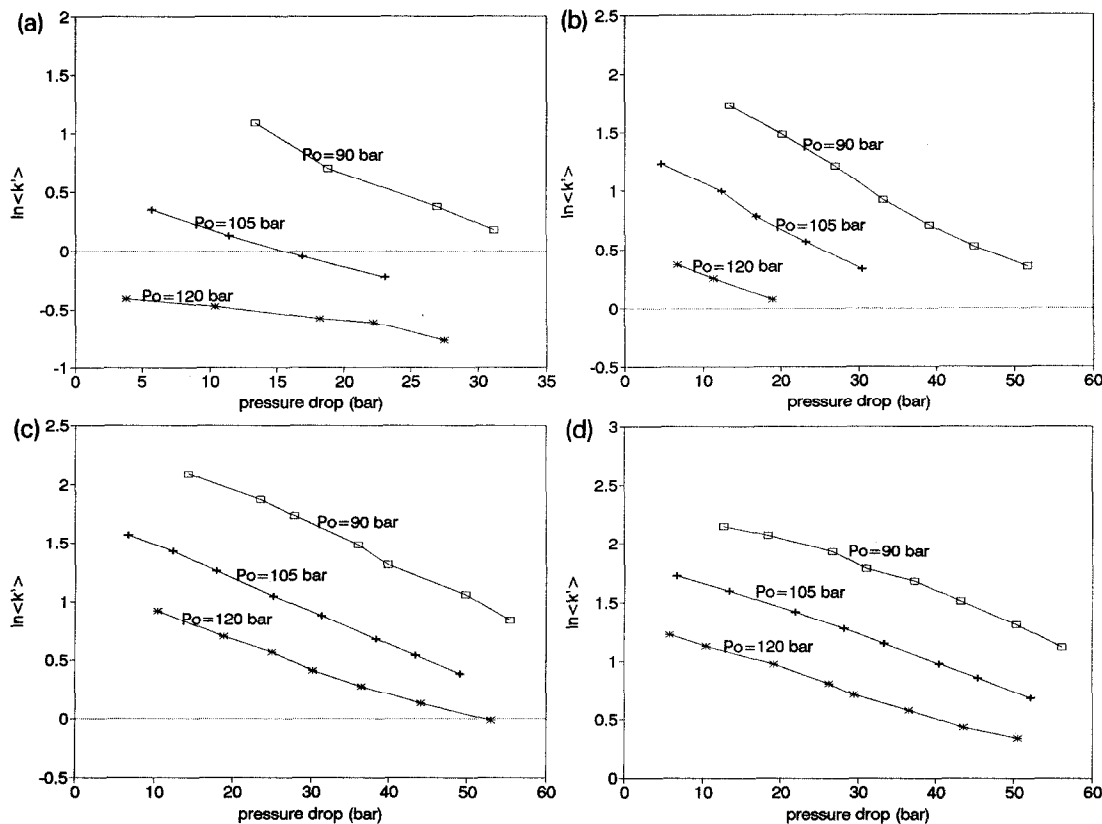
Fig. 1. Plots of the logarithm of the observed capacity factor, ln $\langle k' \rangle$, vs. the pressure drop for ethylbenzene at (a) 50, (b) 60, (c) 70 and (d) 80°C, and the outlet pressure indicated.

column, the temporal average density is always higher than the arithmetic average density (see Table I), and the difference between the arithmetic average density and the temporal average density becomes more significant with a larger pressure drop [8]. At constant arithmetic average density, the temporal average density actually increases with increasing pressure drop. Therefore, at constant arithmetic average density, the observed capacity factor is expected to decrease with pressure drop due to the increase in the temporal average density.

Plots of ln $\langle k' \rangle_{obs}$ vs. pressure drop are illustrated in Fig. 1. Extrapolation of the plots to zero pressure drop presumably gives the ln k' values at the set outlet density for a hypothetical column having zero pressure drop. The logarithm of the observed capacity factor can be empirically fit to a linear function of pressured drop (ΔP), ln $\langle k' \rangle_{obs} = a + b\Delta P$, and the

intercepts are the extrapolated values of ln $\langle k' \rangle_{obs}$ at the outlet density. The extrapolated values of ln $\langle k' \rangle_{obs}$ for ethylbenzene at various outlet densities and temperatures are listed in Table II.

The extrapolated, zero-pressure-drop data approximately represent the local ln k' values at the corresponding (outlet) densities. Incorporating the extrapolated ln k' values into Figs. 2a–5a illustrates that the extrapolated zero-pressure-drop data fall on the curves characterized by the temporal average density. This suggests that the hypothetical curves of local ln k' vs. local density, which are described by eqn. 1 and are supposed to pass through the extrapolated zero-pressure-drop data points, closely match the characterization curves of ln $\langle k' \rangle_{obs}$ vs. the temporal average density, which are expressed by eqn 8. Accordingly, the retention process may be characterized and represented by a hypothetical
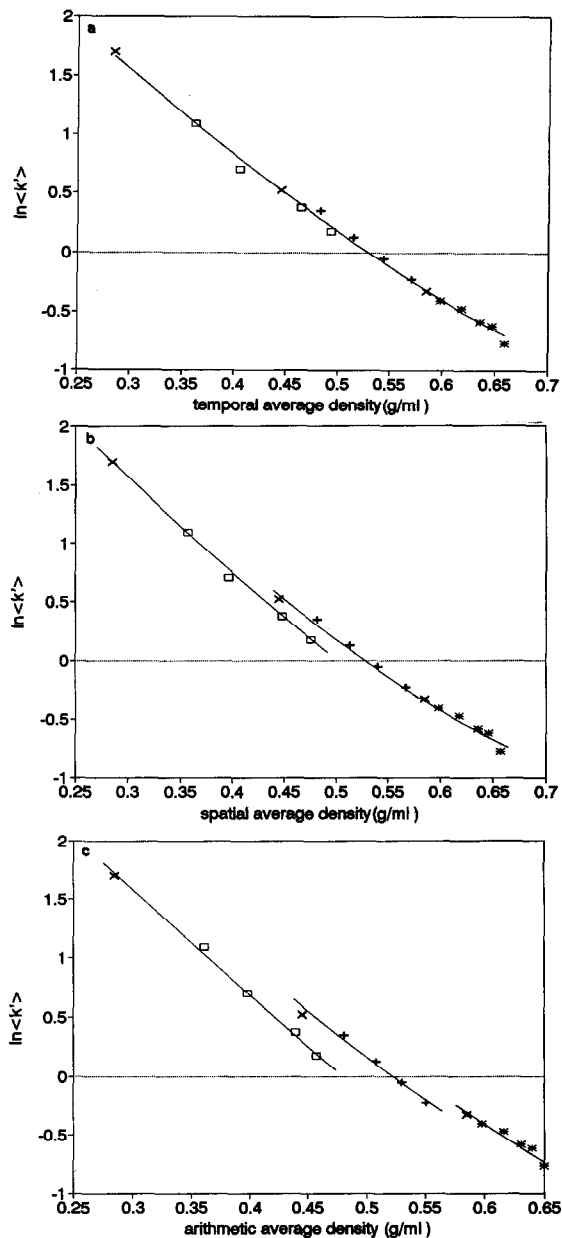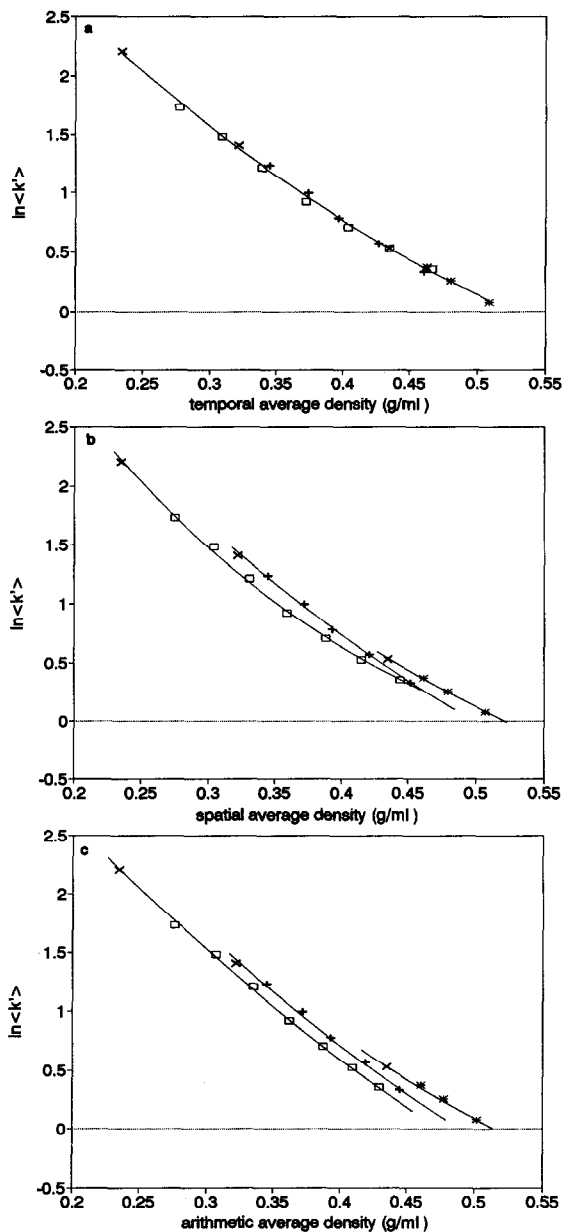
Fig. 2. Plots of the logarithm of the observed capacity factor, ln $\langle k' \rangle$, vs. (a) the temporal average density, (b) the spatial average density and (c) the arithmetic average density, for ethylbenzene at 50°C; × from extrapolation to $\Delta P = 0$. Symbols as in Fig. 1.

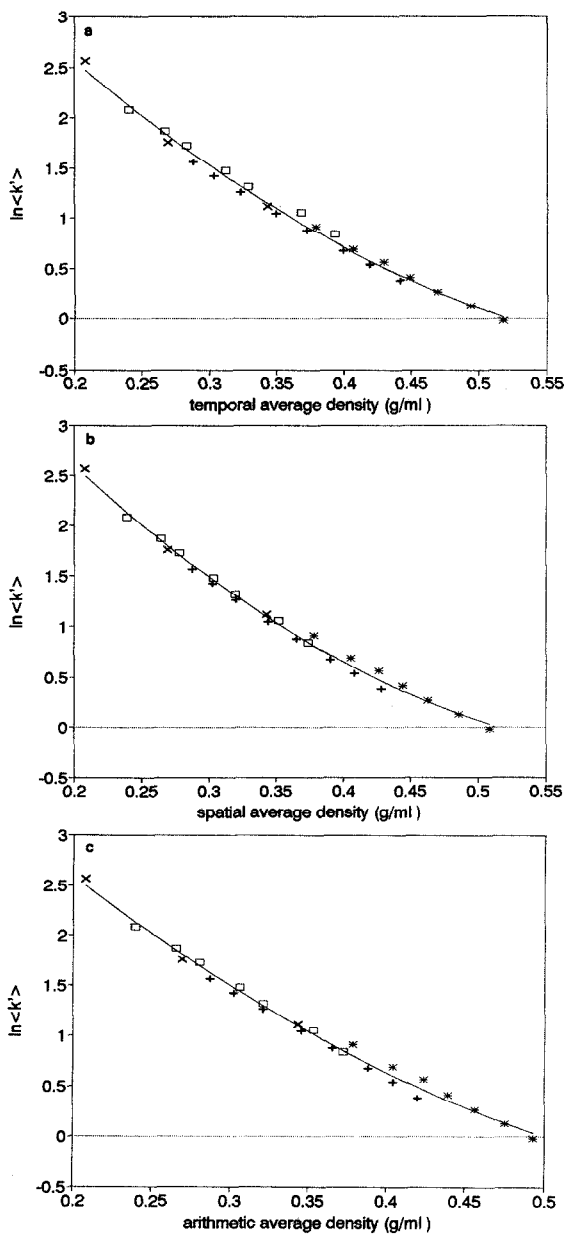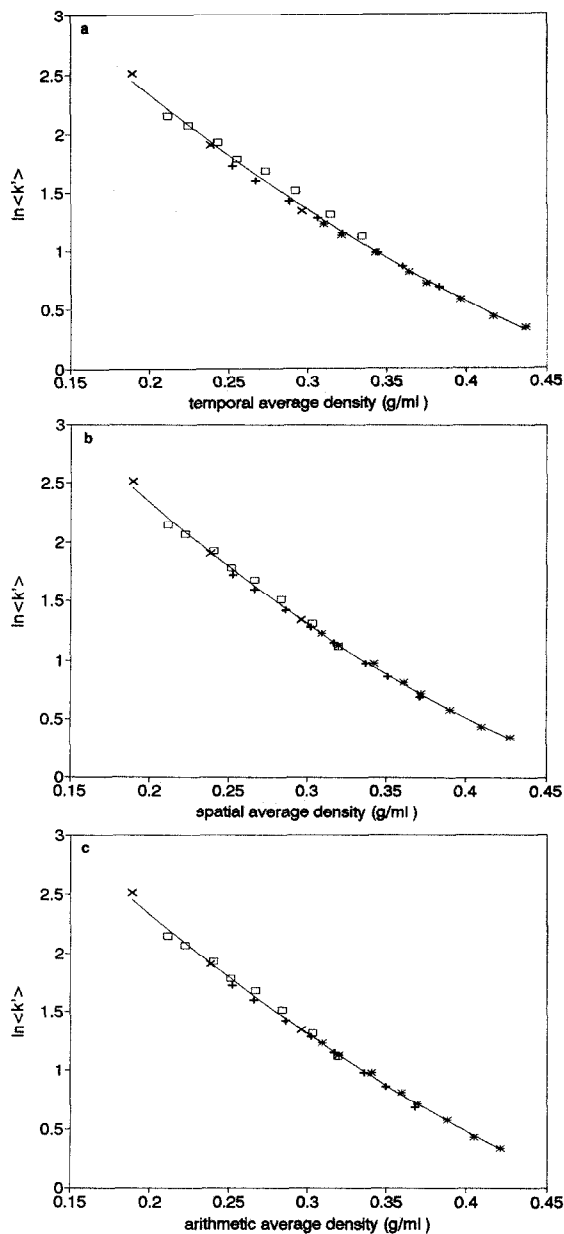Fig. 3. Plots of the logarithm of the observed capacity factor, ln $\langle k' \rangle$, vs. (a) the temporal average density, (b) the spatial average density and (c) the arithmetic average density, for ethylbenzene at 60°C; × from extrapolation to $\Delta P = 0$. Symbols as in Fig. 1.

zero-pressure-drop system at a density equal to the temporal average density of the real system. Therefore, this suggests that, for a packed column SFC system, the fundamental coefficients a, b and c in

eqn. 1 should be essentially equal to the coefficients a', b' and c' in eqn. 8, which may be obtained from the regression of ln $\langle k' \rangle_{obs}$ vs. $\langle \rho \rangle_t$ (see below).

Fig. 6 shows the behavior of homologues. The

Fig. 4. Plots of the logarithm of the observed capacity factor, ln ⟨k'⟩, vs. (a) the temporal average density, (b) the spatial average density and (c) the arithmetic average density, for ethylbenzene at 70°C; × from extrapolation to $\Delta P = 0$. Symbols as in Fig. 1.

Fig. 5. Plots of the logarithm of the observed capacity factor, ln ⟨k'⟩, vs. (a) the temporal average density, (b) the spatial average density and (c) the arithmetic average density, for ethylbenzene at 80°C; × from extrapolation to $\Delta P = 0$. Symbols as in Fig. 1.

vertical distance between the curves of the solutes represents the logarithm of the selectivity factor. As long as the retention process is characterized by the temporal average density, the selectivity will be

unique and exclusive at a given temperature and density, independent of the pressure drop and the outlet pressure.

TABLE II

EXTRAPOLATED LN k' VALUES AT THE VARIOUS OUTLET DENSITIES AND TEMPERATURES FOR ETHYLBENZENE

Temperature (°C)		Outlet pressure (bar)		
		90	105	120
50	ρ_0 (g/ml)	0.285	0.445	0.585
	ln k'	1.695	0.517	−0.331
60	ρ_0 (g/ml)	0.235	0.322	0.435
	ln k'	2.203	1.402	0.531
70	ρ_0 (g/ml)	0.208	0.269	0.343
	ln k'	2.568	1.762	1.117
80	ρ_0 (g/ml)	0.189	0.238	0.296
	ln k'	2.508	1.901	1.341

Fig. 6. The logarithm of the observed capacity factor, ln $\langle k' \rangle$, characterized by the temporal average density for (a) benzene (■), ethylbenzene (▲), n-butylbenzene (✳), and (b) methylbenzene (■) and n-propylbenzene (▲), at 60°C.

DISCUSSION

As indicated, SFC retention described in terms of the temporal average density of the mobile phase is independent of the pressure drop or the ratio of the inlet to the outlet pressure for the column. Since the plots of ln $\langle k' \rangle_{\text{obs}}$ vs. $\langle \rho \rangle_t$ match the presumed plots of local ln k' vs. local density, the true relation between ln k' and local density (eqn. 1) may be represented by the relation between ln $\langle k' \rangle_{\text{obs}}$ and the temporal average density (eqn. 8). Therefore, the temporal average density is the parameter that should be chosen to characterize the retention process.

However, in practical SFC applications, e.g., in SFC methods development, the arithmetic average density is often employed for simplicity. When there is a large density gradient along the column, use of the arithmetic average density to characterize SFC retention may result in large deviations leading to poor reproducibility, since at constant arithmetic average density SFC retention is also a function of the pressure drop. For example, as shown in Fig. 2, at constant temporal average density the observed capacity factor is unique, while at constant arithmetic average density the observed capacity factor can be different, depending on the pressure drop. One way to estimate potential discrepancies from the use of the arithmetic average density in correlating and representing experimental data in packed column SFC systems, instead of using the temporal average density, is to examine the relative deviation of the arithmetic average density from the temporal average density,

$$\Delta(\%) = \left(\frac{\langle \rho \rangle_t - \langle \rho \rangle_a}{\langle \rho \rangle_t} \right) \cdot 100\% \tag{11}$$

The values of the relative deviation $\Delta(\%)$ were calculated as a function of pressure drop at various temperatures. The results are illustrated in Fig. 7, which shows that the relative deviation increases substantially with increasing pressure drop at constant temperature and a constant outlet pressure of 90 bar. For example, it approaches 10% at a practical operating condition of 40 bar in pressure drop, 90 bar in outlet pressure and 50°C. Due to the high compressibility of the supercritical fluid, the deviations become much more significant at lower temperature.
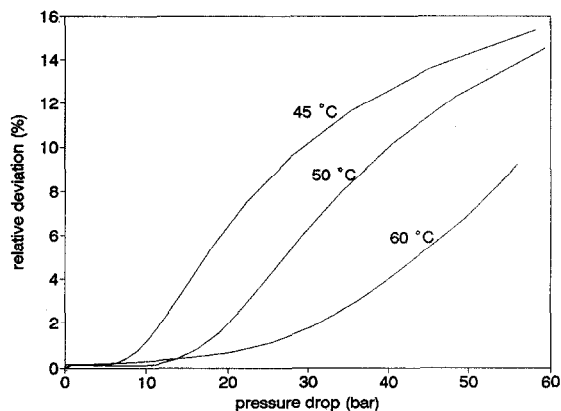
Fig. 7. The relative deviations, defined by eqn. 11, as a function of the pressure drop at an outlet pressure of 90 bar and the temperatures indicated.

The average density depends on the density gradient (density drop and density distribution) along the length of the column and the column temperature. When the density gradient is minimal and/or the density profile is relatively linear, the arithmetic average density, the spatial average density and the temporal average density are nearly identical; therefore, the three forms of density are equally valid in characterizing the observed retention, such as in the folowing cases,

(a) when the pressure drop along the column is small;

(b) when the temperature is substantially higher than the critical temperature [8]; and/or

(c) when the column outlet density is sufficiently greater than the critical density [8].

As mentioned in the introduction, a theoretical linkage between the expression for local retention (eqn. 1) and the expression for observed retention (eqn. 8) is lacking. It has been shown that the observed capacity factor is the temporal averaged one, as expressed by eqn. 7. According to the definition of the temporal average, the observed capacity factor ought to be expressed as

$$\langle k' \rangle_{obs} = \langle k' \rangle_t = \frac{\int_{\rho_o}^{\rho_i} k' D_t(\rho) \, d\rho}{\int_{\rho_o}^{\rho_i} D_t(\rho) \, d\rho}$$

$$= \frac{\int_{\rho_o}^{\rho_i} [\exp(a + b\rho + c\rho^2)] \, D_t(\rho) \, d\rho}{\int_{\rho_o}^{\rho_i} D_t(\rho) \, d\rho}$$

$$= \langle \exp(a + b\rho + c\rho^2) \rangle_t \qquad (12)$$

The observed capacity factors, $\langle k \rangle_{obs}$, were calculated according to eqn. 12, with assumed coefficients a, b and c, and a series of given inlet and outlet densities. However, using the same set of coefficient values as a, b and c in eqn. 12 for a', b' and c' in eqn. 8 (with $\langle \rho \rangle_y = \langle \rho \rangle_t$), the capacity factor calculated from eqn. 12 and the capacity factor calculated from eqn. 8 become obviously different as the pressure drop substantially increases, particularly at 50 and 60°C. There are two possible explanations for this difference.

(1) The mathematical treatment leading to eqn. 12 is rigorous. Therefore, the capacity factor calculated from eqn. 12 should be the true value of the observed capacity factor for the given coefficients a, b and c, and the given inlet and outlet densities, *provided* eqn. 12 can be accurately evaluated numerically. The deviation of the experimentally observed capacity factor from the characteristic value at large pressure drop might then be due to one or more of the following: (a) a thermal non-equilibrium [9] as the highly compressible mobile phase expands from the high density region near the column inlet towards the low density region near the column outlet; (b) a mass-transferal non-equilibrium [11] at large pressure drop and high flow-rate; and (c) turbulent flow in the column. (All the equations for the temporal and spatial parameters are derived based on Darcy's law which is only valid in laminar flow for apparent Reynolds number within an upper limit. The Reynolds numbers for the experiments were calculated, revealing that in some runs with very high flowrates, thus very large pressure drops, they fell in the laminar/turbulent transition region, and therefore, turbulence might be occurring under those conditions.) If the above explanation is valid, the fitting coefficients a', b' and c' from eqn. 8 would not strictly represent the physicochemical parameters for an equilibrium SFC system. Instead, they would reflect the comprehensive effect of both the microscopic molecular interactions and the macroscopic flow dynamics.

(2) If the experimentally measured capacity factor is obtained under near-equilibrium conditions and it is the characteristic value of the system, then the fitting coefficients a', b' and c' from eqn. 8 would have physicochemical significance. The deviation of the capacity factor calculated by eqn. 12 from the experimentally measured capacity factor might then be due to error in implementing the numerical integration of eqn. 12. Involved in the integration of eqn. 12 is the core of the distribution function, $\eta^{-1}(\partial P/\partial\rho)$, which was evaluated using the equation of state and tabulated viscosity data, and fit to a seventh-order polynomial in reduced density at a given temperature [8]. By this method, the numerical integration of eqn. 12 becomes extremely sensitive when the inlet and outlet mobile phase densities fall in the vicinity of the minimum region in the core of the distribution function as a function of density [8], which may result in error in the observed capacity factor calculated by the numerical integration of eqn. 12.

Further investigation of these pressure-drop effects is currently underway.

CONCLUSIONS

This experimental study reveals that, in a packed column SFC system with a large pressure drop, (a) the chromatographic retention of solutes can be best characterized by the temporal average density of the mobile phase at a given temperature, (b) the retention processes may be represented by a hypothetical zero-pressure-drop system at a density equal to the temporal average density of the real system, and (c) when using the temporal average density to characterize the observed retention, physicochemically meaningful parameters a, b and c in the local

retention–local density relations (eqn. 1) *may* be obtainable from the coefficients a, b' and c', by fitting the observed retention as a function of the temporal average density (eqn. 8, with $y = t$).

ACKNOWLEDGEMENTS

REFERENCES

1 D. R. Gere, R. Board and D. McManigill, *Anal. Chem.*, 55 (1983) 1370.
2 D. E. Martire, R. L. Riester and X. Zhang, in F. Bondi and G. Guiochon (Editors), *Theoretical Advancement in Chromatography and Related Separation Techniques*, Kluwer, Dordrecht, in press.
3 D. E. Martire and R. E. Boehm, *J. Phys. Chem.*, 91 (1987) 2433.
4 D. E. Martire, *J. Chromatogr.*, 452 (1988) 17.
5 D. E. Martire and R. E. Boehm, *J. Phys. Chem.*, 87 (1983) 1045.
6 D. E. Martire, *J. Chromatogr.*, 461 (1989) 165.
7 X. Zhang, *Doctoral Dissertation*, Georgetown University, Washington, DC, 1991.
8 D. E. Martire, R. L. Riester, T. J. Bruno, A. Hussam and D. P. Poe, *J. Chromatogr.*, 545 (1991) 135.
9 P. J. Schoenmakers and F. C. C. J. G. Verhoeven, *J. Chromatogr.*, 352 (1986) 315.
10 P. J. Schoenmakers and L. G. M. Uunk, *Chromatographia*, 24 (1987) 51.
11 J. C. Giddings, *Unified Separation Science*, Wiley, New York, 1991.